Int. J. Electrochem. Sci., 7 **(2012)** 89 - 105

International Journal of
ELECTROCHEMICAL
SCIENCE
www.electrochemsci.org

Corrosion Inhibition of Copper in Nitric Acid Solutions Using a New Triazole Derivative

Zarrouk [1], *B. Hammouti* [1], *H. Zarrok* [2], *M. Bouachrine* [3], *K.F. Khaled* [4,5,*], *S.S. Al-Deyab* [6]

[1] LCAE-URAC18, Faculté des Sciences, Université Mohammed I[er], Oujda, Morocco
[2] Laboratoire des procèdes de séparation, Faculté des Sciences, Université Ibn Tofail, Kénitra, Morocco
[3] UMIM, Faculté Polydisciplinaire de Taza, Université Sidi Mohamed Ben Abdellah, Taza, Morocco
[4] Electrochemistry Research Lab., Chemistry Department, Faculty of Education. Ain Shams Univ., Roxy, Cairo, Egypt
[5] Materials and Corrosion Lab., Chemistry Department, Faculty of Science. Taif University, Kingdom of Saudi Arabia
[6] Petrochemical Research Chair, Chemistry Department, College of Science, King Saud University, P.O. Box 2455, Riyadh 11451, Saudi Arabia
[*]E-mail: khaledrice2003@yahoo.com

Received: 14 October 2011 / *Accepted:* 30 November 2011 / *Published:* 1 January 2012

In this study, the inhibition effect of 3-amino-1,2,4-triazole (ATA) on copper corrosion in 2M HNO_3 solution was studied. Electrochemical techniques such as potentiodynamic polarization curves, weight loss (WL) and electrochemical impedance spectroscopy (EIS) were used. Results showed that ATA has good inhibition efficiency on the corrosion of copper in 2M HNO_3 solution. Polarization measurements indicated that, the studied inhibitor acts as a mixed type one. The inhibition efficiency depends on the concentration of inhibitor and reaches 82.2% at 10^{-2}M ATA. The results obtained from the different methods are in good agreement. The adsorption of ATA molecules on the copper surface obeys Langmuir adsorption isotherm. The adsorption free energy of ATA on copper (-29.95 kJ / mol) reveals a physical adsorption of the inhibition on the metal surface. Quantum chemical calculations using DFT at the B3LYP/6-31G* level of theory was further used to calculate some electronic properties of the molecule in order to ascertain any correlation between the inhibitive effect and molecular structure of 3-amino-1,2,4-triazole.

Keywords: Copper; Nitric Acid; Corrosion Inhibition; EIS; Potentiodynamic Polarisation; Weight Loss; DFT.

1. INTRODUCTION

Copper and its alloys are widely used materials for their excellent electrical and thermal conductivities in many applications such as electronics [1] and recently in the manufacture of

integrated circuits [2–4]. Copper is relatively noble metal, requiring strong oxidants for its corrosion or dissolution. The chemical dissolution and electrolytic plating are the main processes used in the fabrication of electronic devices. The most widely used corrosive solution contains nitric acid, so this medium has induced a great deal of research on copper corrosion [5–20]. In order to study the corrosion of metals, several techniques have been applied. The use of chemical inhibitors is one of the most practical methods for the protection against corrosion in acidic media. Most of the excellent acid inhibitors are organic compounds containing nitrogen [21–23], oxygen [24–27], phosphorus [28] and sulphur [29–32]. Studies of the relation between adsorption and corrosion inhibition are of considerable importance. In the present paper, the inhibition of copper corrosion in 2M HNO_3 solutions by 3-amino-1,2,4-triazole (ATA, Figure 1) has been studied.

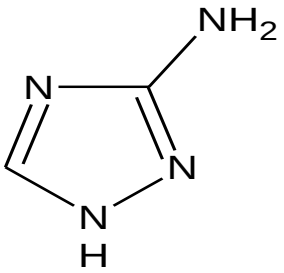

Figure 1. The molecular structure of ATA.

The compound has shown high inhibition efficiency against corrosion of copper in various aggressive media [33-37] due to its adsorption onto the metal surface, because it is a heterocyclic compound containing a variety of donor atoms.

2. EXPERIMENTAL DETAILS

2.1. Materials and reagents

Copper strips containing 99.5 wt.% Cu, 0.001wt.% Ni, 0.019 wt.% Al, 0.004 wt.% Mn, 0.116 wt.% Si and balance impurities were used for electrochemical and gravimetric studies. The Copper samples were mechanically polished using different grades of emery paper, washed with double distilled water, and dried at room temperature. Appropriate concentration of aggressive solutions used (2M HNO_3) was prepared using double distilled water. 3-amino-1,2,4-triazole is Sigma–Aldrich, 99% analytical grade.

2.2. Electrochemical measurements

2.2.1. Electrochemical cell

The electrolysis cell was a pyrex of cylinder closed by cap containing five openings. Three of them were used for the electrodes. The working electrode was copper with the surface area of 0.28

cm^2. Before each experiment, the electrode was polished using emery paper until 2000 grade. After this, the electrode was cleaned ultrasonically with distilled water. A saturated calomel electrode (SCE) was used as a reference. All potentials were given with reference to this electrode. The counter electrode was a platinum plate of surface area of 1 cm^2.

The aggressive medium used here is 2M HNO_3 solution was prepared with concentrated HNO_3 and distilled water. The molecule structure of triazole tested are shown in Fig. 1. The concentration range of this compounds was 10^{-5} to 10^{-2} M.

2.2.2. Polarisation measurements

The working electrode was immersed in test solution during 30 minutes until a steady state open circuit potential (E_{ocp}) was obtained. The polarization curve was recorded by polarization from -150 mV to 150 mV under potentiodynamic conditions corresponding to 1 mV/s (sweep rate) and under air atmosphere. The potentiodynamic measurements were carried out using Tacussel Radiometer PGZ 301, which was controlled by a personal computer.

2.2.3. EIS measurements

The electrochemical impedance spectroscopy measurements were carried out using a transfer function analyzer (Tacussel Radiometer PGZ 301), with a small amplitude ac. Signal (10 mV rms), over a frequency domain from 100 KHz to 10 mHz at 303 K and an air atmosphere. The polarization resistance R_p, is obtained from the diameter of the semicircle in Nyquist representation.

2.3. Weight loss measurements

Gravimetric experiments were carried out in a double walled glass cell. The solution volume was 50 cm^3; the temperature of 303 K was controlled thermostatically. The weight loss of copper in 2M HNO_3 with and without the addition of inhibitor was determined after immersion in acid for 1 h. The copper specimens were rectangular in the form (2 cm ×2 cm × 0.20 cm).

2.4. Computational chemistry

The quantum calculations were performed using the Gaussian 03 program [38]. The geometry of the studied compound was evaluated using the DFT level of the three-parameter compound functional of Becke (B3LYP) [39]. The 6-31G* basis set was used for all atoms [40-43]. The geometry structure was optimized under no constraint. The following quantum chemical indices were considered: the energy of the highest occupied molecular orbital (E_{HOMO}), the energy of the lowest unoccupied molecular orbital (E_{LUMO}), $\Delta E_{gap} = E_{HOMO} - E_{LUMO}$, the dipole moment ($\mu$) and total energy (TE).

3. RESULTS AND DISCUSSION

3.1. Weight loss tests

3.1.1. Effect of concentration

Three parallel rectangular copper specimens were used for the determination of corrosion rate.

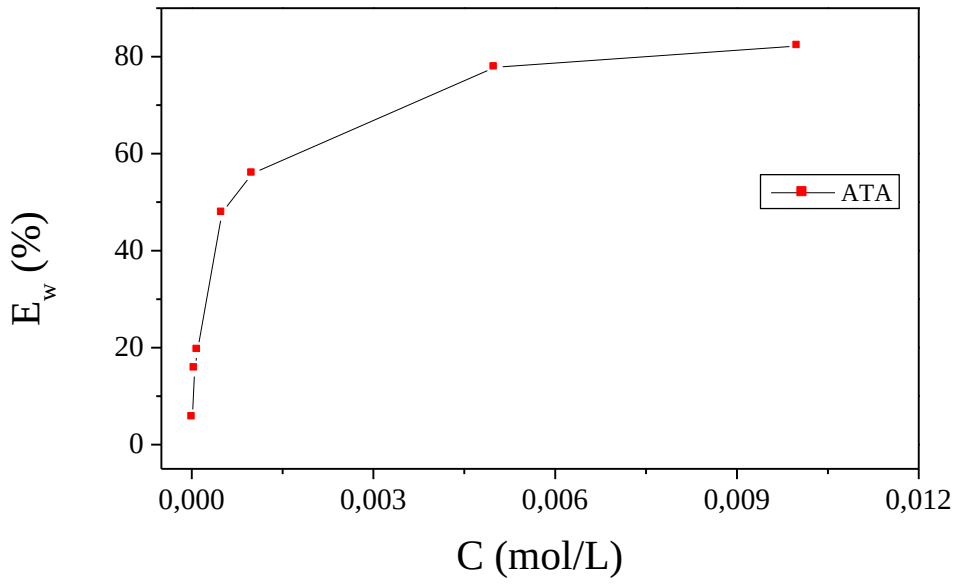

Figure 2. Variation of inhibition efficiency on copper with different concentrations of ATA inhibitor in 2M HNO_3 at 303K for 1h immersion time.

The coupons, initial weight using an analytic balance before immersion in 80 ml open beakers containing 50 ml of corrosive medium (2M HNO_3) without and with different concentrations of ATA. The specimens were taken out, washed, dried, and reweighed accurately. The average weight loss of the three parallel copper specimens could be obtained. The corrosion rates of the copper coupons have been determined for 1h immersion period at 303K from mass loss, using Eq. (1) where Δm is the mass loss, S is the area, and t is the immersion period [44]. The percentage protection efficiency E_w(%) was calculated according the relationship Eq. (2) where W and W_{inh} are the corrosion rates of copper without and with the inhibitor, respectively [45]:

$$W = \frac{\Delta m}{S.t} \quad (1)$$

$$E_w\% = \frac{W - W_{inh}}{W} \quad (2)$$

The value of percentage inhibition efficiency (E_w%) and corrosion rate (CR) obtained from weight loss method at different concentrations of ATA in 2M HNO_3 at 303K are summarized in Table 1.

Table 1. Corrosion parameters for copper in aqueous solution of 2M HNO_3 in absence and presence of different concentrations of ATA from weight loss measurements at 303K for 1h.

Inhibitor	Con (M)	W(mg/cm^2.h)	E_w (%)	Θ
Blank	2 M HNO_3	1.78	-	
ATA	10^{-2}	0.32	82.2	0.822
	5×10^{-3}	0.39	77.9	0.779
	10^{-3}	0.78	55.9	0.559
	5×10^{-4}	0.93	47.9	0.479
	10^{-4}	1.43	19.5	0.195
	5×10^{-5}	1.50	15.7	0.157
	10^{-5}	1.68	05.6	0.056

The variation of inhibition efficiency with increase in inhibitor concentrations is shown in Fig. 2. It was observed that ATA inhibits the corrosion of copper in HNO_3 solution, at all concentrations used in study, i.e. from 10^{-5} M to 10^{-2} M. Maximum inhibition efficiency was shown at 10^{-2} M concentration of the inhibitor in 2M HNO_3 at 303K. It is evident from Table 1 that the corrosion rate is decreased from 1.78 mg/cm^2.h to 0.32 mg/cm^2.h on the addition of 10^{-2}M of ATA.

3.1.2. Adsorption isotherm and thermodynamic activation parameters

In order to study the effect of temperature on the inhibition efficiencies of ATA, weight loss measurements were carried out in the temperature range 303–343K in absence and presence of inhibitor at optimum concentration. The various corrosion parameters obtained are listed in Table 2.

The fractional surface coverage Θ can be easily determined from the weight loss measurements by the ratio E_w%/100, where E_w% is the inhibition efficiency that calculated using relation (1). The data obtained suggests that ATA get adsorbed on the copper surface at all temperatures studied and corrosion rates increased in absence and presence of inhibitor with increasing in temperature in 2M HNO_3 solutions. In acidic media, corrosion of metal is generally accompanied with evolution of H_2 gas; rise in temperature usually accelerates the corrosion reactions which results in higher dissolution rate of the metal.

Inspection of Table 2 showed that corrosion rate increased with increasing temperature both in uninhibited and inhibited solutions while the inhibition efficiency of ATA decreased with temperature. A decrease in inhibition efficiencies with the increase temperature in presence of ATA might be due to weakening of physical adsorption.

Table 2. Various corrosion parameters for copper in 2M HNO_3 in absence and presence of optimum concentration of ATA at different temperatures.

Temperature (K)	Inhibitor	W(mg/cm^2.h)	E_w (%)	Θ
	Blank	1.78	-	-
303	ATA	0.32	82.2	0.822
	Blank	7.33	-	-
313	ATA	2.02	72.5	0.725
	Blank	24.97	-	-
323	ATA	8.43	66.2	0.662
	Blank	70.82	-	-
333	ATA	27.59	61.0	0.610
	Blank	186.61	-	-
343	ATA	12.08	35.6	0.356

In order to calculate activation parameters for the corrosion process, Arrhenius Eq. (3) and transition state Eq. (4) were used [46]:

$$C_R = A\exp\left(\frac{-E_a}{RT}\right) \quad (3)$$

$$C_R = \frac{RT}{Nh}\exp\left(\frac{\Delta S_a^\circ}{R}\right)\exp\left(-\frac{\Delta H_a^\circ}{RT}\right) \quad (4)$$

Where C_R is the corrosion rate, R the gas constant, T the absolute temperature, A the pre-exponential factor, h the Plank's constant and N is Avogrado's number, E_a the activation energy for corrosion process , ΔH_a° the enthalpy of activation and ΔS_a° the entropy of activation.

The apparent activation energie (E_a) at optimum concentration of ATA was determined by linear regression between Ln C_R and 1/T (Fig. 3) and the result is shown in Table 3.

Table 3. Activation parameters E_a, ΔH_a° and ΔS_a° for the copper dissolution in 2M HNO_3 in the absence and the presence of ATA at optimum concentration.

	A (mg/cm^2.h)	Linear regression coefficient (r)	E_a (kJ/mol)	ΔH_a° (kJ/mol)	ΔS_a° (J/mol.K)	K_{ads} (M^{-1})	ΔG°_{ads} (kJ/mol)
Blank	3.6627×10^{17}	0.99908	100.21	097,53	082.36	-	-
ATA	1.3933×10^{21}	0.99860	125.26	122,58	150.89	2623.69	-29.95

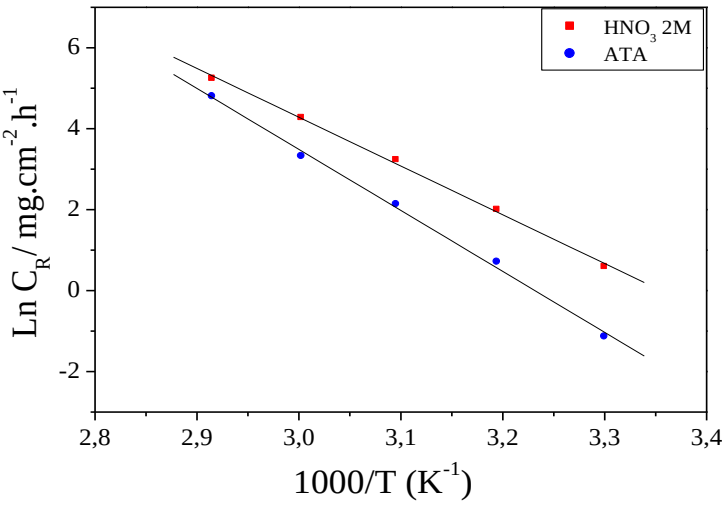

Figure 3. Arrhenius plots of log C_R vs. 1/T for copper in 2M HNO_3 in the absence and the presence of ATA at optimum concentration.

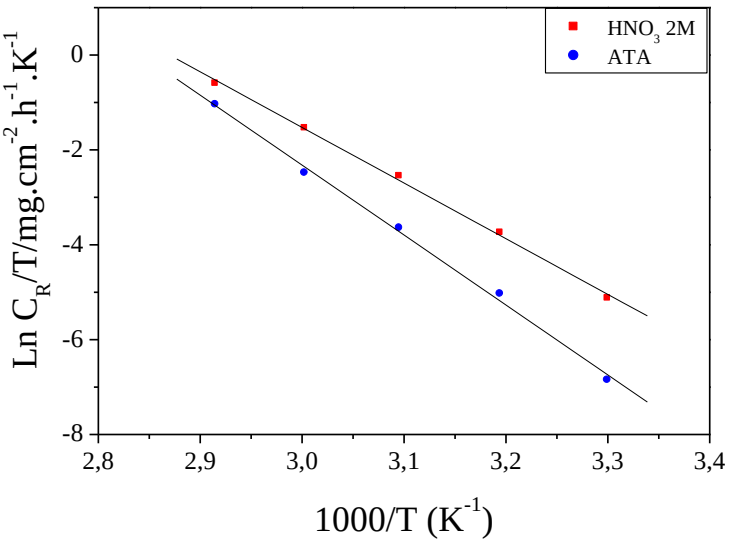

Figure 4. Arrhenius plots of log C_R/T vs. 1/T for copper in 2M HNO_3 in the absence and the presence of ATA at optimum concentration.

The linear regression coefficient was close to 1, indicating that the copper corrosion in nitric acid can be elucidated using the kinetic model. Inspection of Table 3 showed that the value of E_a determined in 2M HNO_3 containing ATA is higher (125.26 kJ mol^{-1}) than that for uninhibited solution (100.21 kJ mol^{-1}). The increase in the apparent activation energy may be interpreted as physical adsorption that occurs in the first stage [47]. Szauer and Brand explained the increase in activation energy due to an appreciable decrease in the adsorption of the inhibitor on the copper surface with increase in temperature. As adsorption decreases more desorption of inhibitor molecules occurs because these two opposite processes are in equilibrium. Due to more desorption of inhibitor

molecules at higher temperatures the greater surface area of copper comes in contact with aggressive environment, resulting increased corrosion rates with increase in temperature [48].

Fig. 4 showed a plot of Ln (C_R/T) versus 1/T. The straight lines are obtained with a slope (ΔH_a° /R) and an intercept of (Ln R/Nh + $\Delta S°_a$ /R) from which the values of the values of ΔH_a° and ΔS_a° are calculated and are given in Table 3. Inspection of these data revealed that the thermodynamic parameters (ΔH_a° and ΔS_a°) for dissolution reaction of copper in 2M HNO_3 in the presence of ATA is higher (122.58 kJ mol^{-1}) than that of in the absence of inhibitors (97.53 kJ mol^{-1}). The positive sign of ΔH_a° reflect the endothermic nature of the copper dissolution process suggesting that the dissolution of copper is slow [49] in the presence of inhibitor.

The entropy of activation ΔS_a° in the absence of inhibitor is positive and this value increases positively with the ATA. The increase of ΔS_a° implies that an increase in disordering takes place on going from reactants to the activated complex [50].

3.1.3. Adsorption isotherm

The adsorption isotherm can be determined by assuming that inhibition effect is due mainly to the adsorption at metal/solution interface. Basic information on the adsorption of inhibitors on the metal surface can be provided by adsorption isotherm. In order to obtain the isotherm, the fractional surface coverage values (Θ) as a function of inhibitor concentration must be obtained. The values of Θ can be easily determined from the weight loss measurements by the ratio E_W%/100, where E_W% is inhibition efficiency obtained by weight loss method. So it is necessary to determine empirically which isotherm fits best to the adsorption of inhibitors on the copper surface. Several adsorption isotherms (viz., Frumkin, Langmuir, Temkin, Freundlich) were tested and the Langmuir adsorption isotherm was found to provide the best description of the adsorption behaviour of this inhibitor. The Langmuir isotherm is given by following equation [51]:

$$\frac{\Theta}{1-\Theta} = K_{ads}C \tag{5}$$

The rearrangement gives the following equation : $\frac{C}{\Theta} = \frac{1}{K_{ads}} + C$ (6)

Where C is the concentration of inhibitor, K_{ads} is the equilibrium constant of the adsorption process, and Θ is the surface coverage.

Plot C/Θ versus C yield a straight line (Fig. 5) with regression coefficient, R^2, almost equal to 1. This suggests that ATA in present study obeyed the Langmuir isotherm and there is negligible interaction between the adsorbed molecules. Free energy of adsorption was calculated using the relation [52]:

$$K_{ads} = \frac{1}{55.55} \exp\left(-\frac{\Delta G^{\circ}_{ads}}{RT}\right) \quad (7)$$

Where R is the universal gas constant and T is the absolute temperature. The value 55.55 in the above equation is the concentration of water in solution in mol L^{-1}.

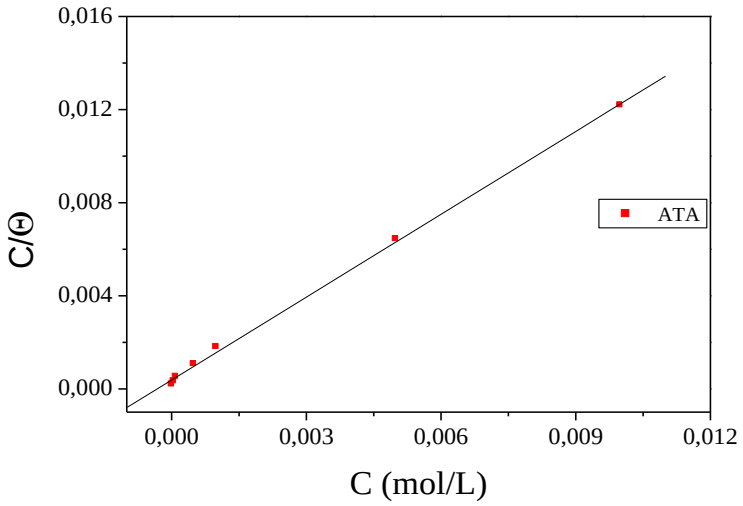

Figure 5. Langmuir isotherm adsorption model of ATA on the surface of copper in 2M HNO_3.

The values of K_{ads} and ΔG°_{ads} were calculated at 303K and are listed in Table 3. The standard free energy of adsorption (ΔG°_{ads}), calculated from Eq. (7), is -29.95 kJ mol^{-1} (K_{ads} = 2623.69 L mol^{-1}). The negative value of the standard free energy of adsorption and the high values of the adsorption constant indicate a spontaneous adsorption of this inhibitor on copper. This means that the inhibitive action of this substance result from the physical adsorption of these molecules on the surface of copper. This is also supported by the fact that the inhibition efficiency of the investigated inhibitor decreases at higher temperature (343K).

3.2. Potentiodynamic polarization measurements

Current–potential characteristics resulting from cathodic and anodic polarisation curves of copper in 2M HNO_3 in the absence and presence of ATA at various concentrations are presented in Fig. 6. Table 4 gives values of corrosion current (I_{corr}), corrosion potential (E_{corr}), catholic Tafel slope (β_c) for ATA at various concentrations in 2M HNO_3. In the case of polarisation method the relation determines the inhibition efficiency (E_I%):

$$E_I\% = \left(1 - \frac{I_{corr}}{I^{\circ}_{corr}}\right) \times 100 \quad (8)$$

Where $I°_{corr}$ and I_{corr} are the uninhibited and inhibited corrosion current densities, respectively, determined by extrapolation of catholic Tafel lines to corrosion potential.

Table 4. Corrosion data of copper in 2M HNO_3 with and without ATA.

Inhibitor	Conc (M)	E_{corr} (mV/ECS)	$-\beta_c$ (mV/dec)	I_{corr} ($\mu A/m^2$)	E_I (%)
Blank	2	34.0	304.7	365.1	-
ATA	10^{-2}	39.5	301.4	095.3	73.9
	5×10^{-3}	41.3	300.5	117.4	67.8
	10^{-3}	40.1	303.9	184.7	49.4
	10^{-4}	21.1	274.1	290.7	20.4
	10^{-5}	35.2	271.9	334.6	08.3

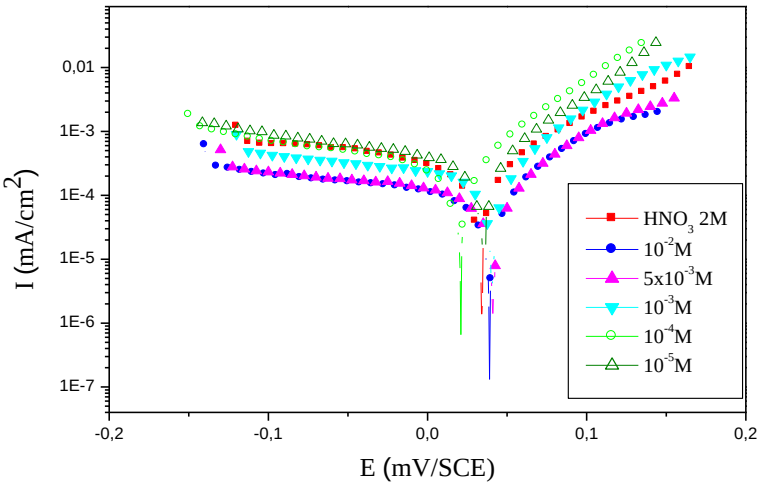

Figure 6. Polarisation plots of copper in 2M HNO_3 for various concentrations of ATA.

As it is show in Fig. 6 and Table 4, cathodic current–potential curves give rise to parallel Tafel lines indicating that the hydrogen evolution reaction is under activation controlled. The cathodic current density decreases with the concentration of ATA however, a slight effect is observed on the anodic portions. This result indicates that ATA is adsorbed on the metal surface on the cathodic sites and hence inhibition occurs. These results demonstrate that the hydrogen reduction is inhibited and that the inhibition efficiency increases with inhibitor concentration to attain 74 % at 10^{-2} M of ATA. We remark that the inhibitor acts on the anodic portion and the anodic current density is reduced (Fig. 6). It seems also that the presence of the inhibitor change slightly the corrosion potential values in no definite direction. These results indicated that ATA acts as a mixed-type inhibitor.

The well known Pourbaix diagram for copper-water system, indicates that copper is corroded to Cu^{2+} in HNO_3 solutions, and no oxide film is formed to protect the surface from corrosion. Copper dissolution is thus expected to be the dominant reaction in HNO_3 solutions.

The pure nitric acid and inhibitor-containing nitric acid solutions used in our experiments were all aerated where dissolved oxygen may be reduced on copper surface and this will allow some copper corrosion to occur [53-55].

It is a good approximation to ignore the hydrogen evolution reaction and only consider oxygen reduction in the aerated nitric acid solutions at potentials near the corrosion potential [56]. Cathodic reduction of oxygen can be expressed either by a direct $4e^-$ transfer, Eq. 9:

$$O_2 + 4H^+ + 4e^- \rightarrow 2H_2O \qquad (9)$$

or by two consecutive $2e^-$ steps involving a reduction to hydrogen peroxide first, Eq. 10, followed by a further reduction, according to Eq. 11 [57]:

$$O_2 + 2H^+ + 2e^- \rightarrow H_2O_2 \qquad (10)$$

$$H_2O_2 + 2H^+ + 2e^- \rightarrow 2H_2O \qquad (11)$$

The transfer of oxygen from the bulk solution to the copper/solution interface will strongly affect rate of oxygen reduction reaction, despite how oxygen reduction takes place, either in $4e^-$ transfer or two consecutive $2e^-$ transfer steps. Dissolution of copper in nitric acid is described by the following two continuous steps:

$$Cu - e^- = Cu(I)_{ads} \quad \text{(fast step)} \qquad (12)$$

$$Cu(I)_{ads} - e^- = Cu(II) \quad \text{(slow step)} \qquad (13)$$

where $Cu(I)_{ads}$ is an adsorbed species at the copper surface and does not diffuse into the bulk solution [58,59]. The dissolution of copper is controlled by the diffusion of soluble Cu(II) species from the outer Helmholtz plane to the bulk solution.

Upon addition of ATSA, it is obvious that the slopes of the anodic (β_a) and cathodic (β_c) Tafel lines remain almost unchanged, giving rise to a nearly parallel set of anodic lines, and an almost parallel cathodic plots results too.

Thus the adsorbed inhibitor act by simple blocking of the active sites for both anodic and cathodic processes.

In other words, the adsorbed inhibitor decreases the surface area for corrosion without affecting the corrosion mechanism of copper in these solutions, and only causes inactivation of a part of the surface with respect to the corrosive medium [61,62].

3.3. Electrochemical impedance spectroscopy

The impedance behaviour of copper, after 30 min of immersion in 2 M HNO_3 solutions without and with various concentrations of ATA, was studied. Measurements were conducted under the respective corrosion potentials at 303 K; results obtained are depicted in Fig. 7. The recorded impedance spectra are, in all cases, characterized by the appearance of two clearly resolved time constants related to the capacitive loop in the high frequency (HF) range and an inductive loop in the low frequency (LF) range. The capacitive loop was related to charge-transfer in corrosion process [62]. The depressed form of the higher frequency loop reflects the surface inhomogeneity of structural or interfacial origin, such as those found in adsorption processes [63]. The presence of the LF inductive RL-L loop may be attributed to the relaxation process obtained by adsorption species like H_{ads}^{+} on the electrode surface. It may also attribute to the re-dissolution of the passivated surface at low frequencies [64].

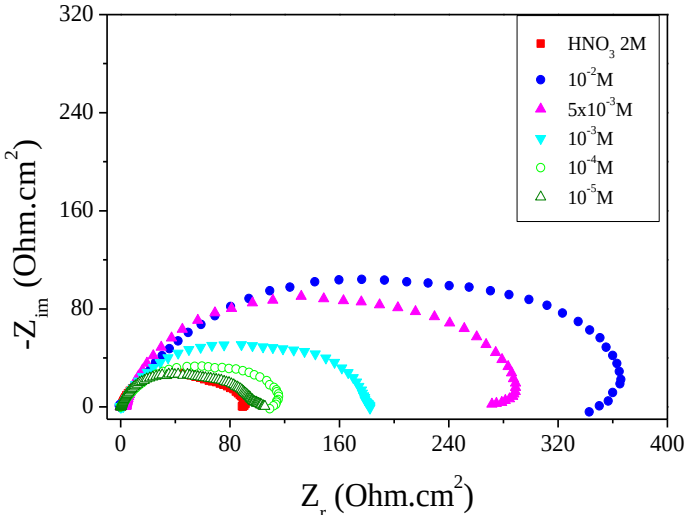

Figure 7. Nyquist plots of copper in 2M HNO_3 containing various concentration of ATA.

Indeed, the impedance behaviour of copper in HNO_3 solutions is somewhat similar to that of copper in H_2SO_4 and HCl solutions [65]. The anodic dissolution of copper in the halide-containing solutions has been proved to be diffusion limited [66] . The diffusion step was due to the transport of CuX_2^- to the bulk solution [40]. However, the corrosion reaction of copper in halide solutions at E_{corr} is composed of the oxidation of copper and the reduction of oxygen dissolved in the solutions [67], these two half reactions also expected to occur in aerated HNO_3 solutions. The increase in the size of the capacitive loop with the addition of ATA molecules show that a barrier gradually forms on the copper surface. The barrier is probably related to the formation of an inhibitor surface film on the electrode surface.

It is well-known that it is essential to develop the appropriate models for the impedance which can then be used to fit the experimental data and extract the parameters which characterize the corrosion process. Indeed, we tried with many suggested equivalent circuits to fit our impedance data

using computer program EQUIVCRT [42]. However, unfortunately, we failed to get a good fitting with our results. It seems that our impedance data are rather complicated (may be due to the formation of two time constants), and require further investigation, in a separate paper, to get the suitable equivalent circuits. Moreover, the diameter of the HF capacitive loop cannot be taken as an accurate measure of the charge-transfer resistance, R_{ct}, since the HF capacitive is composed of two not clearly resolved time constants. These were the reasons why we could not present here a Table including the impedance parameters extracted, using appropriate equivalent circuits, from the recorded impedance data. However, we introduced here the results of impedance to support results obtained from polarization and weight loss measurements, that ATA inhibits the nitric acid corrosion of copper. This is clearly seen from Fig. 7 that the shapes of the impedance plots for inhibited electrodes are not substantially different from those of uninhibited electrodes. The presence of ATA increases the impedance (i.e., size of the capacitive loop) but does not change other aspects of the behaviour. This means, as previously mentioned, that the inhibitor does not alter the electrochemical reactions responsible for corrosion. It inhibits corrosion primarily through its adsorption on the metal surface.

3.4. Theoretical calculations

Quantum chemical methods have already proven to be very useful in determining the molecular structure as well as elucidating the electronic structure and reactivity [68]. Thus, it has become a common practice to carry out quantum chemical calculations in corrosion inhibition studies. The predicted properties of reasonable accuracy can be obtained from density functional theory (DFT) calculations [69,70].

Some quantum chemical parameters, which influence the electronic interaction between surface atoms and inhibitor, are the energy of highest occupied molecular orbital (E_{HOMO}), the energy of lowest unoccupied molecular orbital (E_{LUMO}), the energy gap E_{HOMO}- E_{LUMO} (ΔE), dipole moment (μ) and total energy (TE). All quantum chemical properties were obtained after geometric optimization with respect to the all nuclear coordinates using Kohn–Sham approach at DFT level. The optimized structure of ATA compound as shown in Fig. 8.

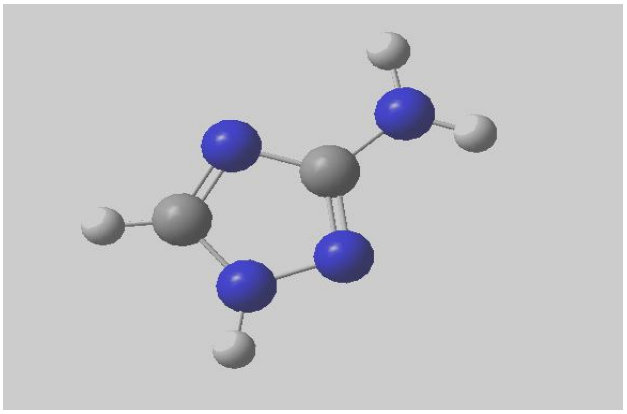

Figure 8. Optimised structure of the studied molecule obtained by B3LYP-6-31 G(d) method.

Table 5. Quantum parameters of ATA calculated with B3LYP/6-31G*

Compound	TE (eV)	E_{HOMO} (eV)	E_{LUMO} (eV)	ΔE_{gap} (eV)	μ (Debye)
ATA	-8092.4984	-6.100144	-0.3468	5.7528	1.3817

The computed quantum chemical properties such as energy of highest occupied molecular orbital (E_{HOMO}), energy of lowest unoccupied molecular orbital (E_{LUMO}), HOMO–LUMO energy gap (ΔE_{H-L}), dipole moment (μ) and total energy (TE) are summarized in the Table 5. As E_{HOMO} is often associated with the electron donating ability of a molecule, high values of E_{HOMO} are likely to indicate a tendency of the molecule to donate electrons to appropriate acceptor molecules with low-energy, empty molecular orbital. Increasing values of the E_{HOMO} facilitate adsorption (and therefore inhibition) by influencing the transport process through the adsorbed layer. Therefore, the energy of the E_{LUMO} indicates the ability of the molecule to accept electrons; hence these are the acceptor states. The lower the value of E_{LUMO}, the more probable, it is that the molecule would accept electrons [71]. As for the values of ΔE (E_{LUMO} - E_{HOMO}) concern; lower values of the energy difference ΔE will cause higher inhibition efficiency because the energy to remove an electron from the last occupied orbital will be low [72]. For the dipole moment (μ), lower values of μ will favor accumulation of the inhibitor in the surface layer.

As we know, frontier orbital theory is useful in predicting the adsorption centers of the inhibitors responsible for the interaction with surface metal atoms. The HOMO and the LUMO population of ATA were plotted and are shown in Fig. 9. Analysis of this figure shows that the density of LUMO is mainly localized on the NH_2 substituent in position 3, while the density HOMO was distributed around the entire molecule.

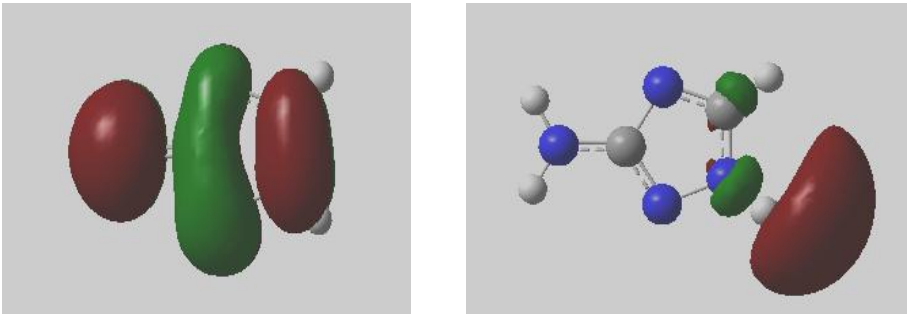

Figure 9. The frontier molecule orbital density distributions of ATA: HOMO (right); LUMO (left).

Moreover, the gap between the LUMO and HOMO energy levels of the molecule was another important factor that should be considered. It has been reported that excellent corrosion inhibitors are usually those organic compounds that are not only offer electrons to unoccupied orbital of the metal but also accept free electrons from the metal [73]. It is also well documented in literature that the higher the HOMO energy of the inhibitor, the greater its ability of offering electrons to unoccupied d-orbital of the metal, and the higher the corrosion inhibition efficiency. It is evident from Table 5 that

ATA has the highest E_{HOMO} in the neutral form. This confirms the experimental results that interaction between ATA and copper is electrostatic in nature (physisorption). In addition, the lower the LUMO energy, the easier the acceptance of electrons from metal surface, as the LUMO-HOMO energy gap decreased and the efficiency of inhibitor improved. It is clear from Table 5 that the ELUMO of ATA exhibits the lowest , making the protonated form the most likely form for the interaction of copper with ATA molecule. Low values of the energy gap (ΔE) will provide good inhibition efficiencies, because the excitation energy to remove an electron from the last occupied orbital will be low [71]. The total energy of the ATA is equal to -8092.4984 eV. This result indicated that ATA is favourably adsorbed through the active centers of adsorption. Lower values of dipole moment (μ) will favour accumulation of the inhibitor in the surface layer and therefore higher inhibition efficiency [74].

Conclusions

- ✓ Results obtained from the experimental and theoretical data show that ATA acts as an effective inhibitor for copper corrosion in nitric acid.
- ✓ The corrosion process was inhibited by adsorption of the organic matter on the copper surface.
- ✓ Inhibition efficiency increases with increase in the concentration of the ATA but decreases with rise in temperature.
- ✓ The adsorption of ATA on copper surface from 2M HNO_3 obeys the Langmuir adsorption isotherm.
- ✓ Phenomenon of physical adsorption is proposed from the values of kinetic / thermodynamics parameters (E_a, ΔG°_{ads}) obtained.
- ✓ Polarisation measurements show that ATA acts essentially as a mixed type inhibitor.
- ✓ The inhibitor efficiency determined by electrochemical polarisation, electrochemical impedance spectroscopy and by gravimetric methods are in good agreement.

ACKNOWLEDGEMENTS

Two of the authors (Prof S. S. Deyab and Prof B. Hammouti) extend their appreciation to the Deanship of Scientific Research at king Saud University for funding the work through the research group project.

References

1. V. Oteino-Alergo, N. Huynh, T. Notoya, S. E. Bottle, D. P. Schwcinsberg, Corros. Sci., 41 (1999) 685.
2. H. Y. Tsai, S. C. Sun, S. J. Wang, J Electrochem Soc., 147 (2000) 2766.
3. A. Krishnamoorthy, K. Chanda, S. P. Murarka, G. Ramanath, J. G. Ryan, Appl Phys Lett., 78 (2001) 2467-2469.
4. C. E. Ho, W. T. Chen, C. R. Kao, J Electron Mater, 30 (2001) 379.

5. U. R. Evans, Trans Farad Soc., 40 (1944)120.
6. A. I. Krosilshchikov, I. V. Dedova, J Gen Chem U.S.S.R., 16 (1946) 537.
7. Y. Komuro, J Chem Soc Jpn., 75 (1954) 255.
8. E. A. Travincek, J. H. Weber, J Phys Chem., 65 (1961) 235.
9. I. S. Smol'yaninov, I. Voronezhsk, Gos Ped Inst., 47 (1964) 34.
10. A. Rasheed Arain A. M. Shams El Din, Thermochim Acta, 89 (1985) 171.
11. A. Zarrouk, A. Dafali, B. Hammouti, H. Zarrok, S. Boukhris, M. Zertoubi, Int. J. Electrochem. Sci., 5 (2010) 46
12. A.Zarrouk, T. Chelfi, A. Dafali, B. Hammouti, S.S. Al-Deyab, I. Warad, N. Benchat, M. Zertoubi, Int. J. Electrochem. Sci., 5 (2010) 696.
13. A. Zarrouk, I. Warad, B. Hammouti, A Dafali, S.S. Al-Deyab, N. Benchat, Int. J. Electrochem. Sci., 5 (2010) 1516.
14. A. Zarrouk, B. Hammouti, A. Dafali, H. Zarrok, Der Pharma Chemica., 3 (2011) 266.
15. A.S. Fouda, H. A. Wahed, Arab. J. Chem., (2011) Article in press.
16. A.S. Fouda, M. M. Gouda and S. I. Abd El-Rahman, Bull. Korean Chem. Soc., 21 (2000) 1085.
17. K. F. Khaled, Mohammed A. Amin, Corros. Sci., 51 (2009) 2098.
18. K. F. Khaled, Sahar A. Fadl-Allah, B. Hammouti, Mater. Chem. Phys., 117 (2009) 148.
19. M. Mihit, K. Laarej, H. Abou El Makarim, L. Bazzi, R. Salghi, B. Hammouti, Arab. J. Chem., 3(2010) 55.
20. A. Fiala, A. Chibani, A. Darchen, A. Boulkamh, K. Djebbar, Appl. Surf. Sci., 253 (2007) 9347.
21. B. A. Abd-EI-Nabey, E. Khamis, M. Sh. Ramadan, A. EI-Gindy , Corrosion, 52 (1996) 671.
22. M. A. Quraishi, D. Jamal, Corrosion, 56 (2000)156.
23. M. Lagrene´e , B. Memaru , N. Chaibi, M. Traisnel , H. Vezin , F. Bentiss, Corros Sci., 43(2001) 951.
24. S. S. Abd EI-Rehim, M. lbrahim, K.F. Khaled, J Appl Electrochem., 29 (1999)593.
25. F. Bentiss, M. Traisnel, L. Gengembre, M. Lagrene´e, Appl Surf Sci., 152 (1999) 237-249.
26. M. G. Hosseini, S. F. L. Mertens, M. Ghorbani, M. R. Arshadi, Mater Chem Phys., 78 (2003) 800.
27. M. Migahed , H. M. Mohamed, A. M. AI-Sabagh, Mater Chem Phys., 80 (2003)169.
28. E. Khamis, E. S. H. EI-Ashry , A. B. Ibrahim, Br Corros J., 35 (2000)150.
29. M. A. Quraishin, H. K.Sharma, Mater Chem Phys., 78 (2002) 18-21.
30. A. Popova, E. Sokolova, S. Raicheva, M. Christov, Corros Sci., 45(2003) 33-58.
31. M. A. Quaraishi, J. Rawat, Mater Chem Phys., 77 (2002) 43.
32. M. El Azhar, B. Memari, M. Traisnel, F. Bentiss, M. Lagrene´e, Corros Sci., 43(2001) 2229.
33. M. S. El-Sayed, R.M. Erasmus, J.D. Comins, J. Colloid Interface Sci., 311 (2007) 144.
34. L. Malki Alaoui, B. Hammouti, A. Bellaouchou, A. Benbachir, A. Guenbour, S. Kertit, Der Pharma Chemica, 3 (2011) 353.
35. Z. Khiati, A.A. Othman, M. Sanchez-Moreno, M.-C. Bernard, S. Joiret, E.M.M. Sutter, V. Vivier, Corros. Sci., 53 (2011) 3092.
36. S. El Issami, L. Bazzi, M. Hilali, R. Salghi, S. Kertit, Ann. Chim. Sci. Mat., 27 (2002) 63.
37. B. Trachli, M. Keddam, H. Takenouti, A. Srhiri, Corros. Sci., 44 (2002) 997.
38. M. J. Frisch, G.W. Trucks, H.B. Schlegel, G.E. Scuseria, M.A. Robb, J.R. Cheeseman, J.A. Montgomery, T. Vreven, Jr., K.N. Kudin, J.C. Burant, J.M. Millam, S.S. Iyengar, J. Tomasi, V. Barone, B. Mennucci, M. Cossi, G. Scalmani, N. Rega, G.A. Petersson, H. Nakatsuji, M. Hada, M. Ehara, K. Toyota, R. Fukuda, J. Hasegawa, M.Ishida, T. Nakajima, Y. Honda, O. Kitao, H. Nakai, M. Klene, X. Li, J.E. Knox, H.P. Hratchian, J.B. Cross, C. Adamo, J. Jaramillo, R.Gomperts, R.E. Stratmann, O. Yazyev, A.J. Austin, R. Cammi, C. Pomelli, J.W. Ochterski, P.Y. Ayala, K. Morokuma, G.A. Voth, P. Salvador, J.J. Dannenberg, V.G. Zakrzewski, S. Dapprich, A.D. Daniels, M.C. Strain, O. Farkas, D.K. Malick, A.D. Rabuck, K. Raghavachari, J.B. Foresman, J.V. Ortiz, Q. Cui, A.G. Baboul, S. Clifford, J. Cioslowski, B.B. Stefanov, G. Liu, A. Liashenko, P. Piskorz, I. Komaromi, R.L. Martin, D.J. Fox, T. Keith, M.A. Al- Laham, C.Y. Peng, A. Nanayakkara, M.

Challacombe, P.M.W. Gill, B. Johnson, W. Chen, M.W. Wong, C. Gonzalez, J.A. Pople, GAUSSIAN 03, Revision B.04, Gaussian, Inc., Pittsburgh PA, 2003.
39. A.D. Becke, J. Chem. Phys., 98 (1993) 5648.
40. J. S. Binkley, J. A. Pople, and W. J. Hehre, J. Am. Chem. Soc., 102 (1980) 939.
41. K. D. Dobbs and W.J. Hehre, J. Comp. Chem., 7 (1986) 359.
42. W. J. Pierto, M. M. Francl, W.J. Hehre, D.J. Defrees, J.A. Pople, J.S. Binkley, J. Am. Chem. Soc., 104 (1982)5039.
43. K. D. Dobbs, W. J. Hehre, J. Comp. Chem., 8 (1987) 880.
44. A.K. Maayta, N.A.F. Al-Rawashded, Corros. Sci., 46 (2004) 1129.
45. K.C. Emreg¨ul, A.A. Akay, O. Atakol, Mater. Chem. Phys., 93 (2005) 325.
46. J.O'M. Bockris, A.K.N. Reddy, Modern Electrochemistry, vol. 2, Plenum Press, New York, 1977. p. 1267.
47. S. Martinez, I. Stern, Appl. Surf. Sci., 199 (2002) 83.
48. T. Szauer, A. Brand, Electrochim. Acta, 26 (1981) 1219.
49. N.M. Guan, L. Xueming, L. Fei, Mater. Chem. Phys., 86 (2004) 59.
50. I.N. Putilova, S. A. Balezin, V. P. Barannik, Metallic Corrosion Inhibitors, Pergamon Press, Oxford, (1960).
51. S. Bilgic, N. Caliskan, Appl. Surf. Sci., 152 (1999) 107.
52. E. Khamis, Corrosion, 46 (1990) 476.
53. R. Schumacher, A. Muller and W. Stockel J. Electroanal. Chem., 219 (1987) 311.
54. W.D. Bjorndahl and K. Nobe Corrosion, 40 (1984) 82.1
55. G. Quartarone, G. Moretti, T. Bellomi, G. Capobianco and A. Zingales Corrosion, 54 (1998) 606.
56. W.H. Smyrl In: J.O'M. Bockris, B.E. Conway, E. Yeager and R.E. White, Editors, Comprehensive Treatise of Electrochemistry Vol. 4, Plenum Press, New York (1981) 116.
57. P. Jinturkar, Y.C. Guan and K.N. Han Corrosion, 54 (1984) 106.
58. T. Hurlen, G. Ottesen and A. Staurset Electrochim. Acta, 23 (1978) 23
59. R. Caban and T.W. Chapman J. Electrochem. Soc., 124 (1977) 1371
60. K.F.Khaled and Amn A. M Corros. Sci., 51 (2009) 2098
61. J.W. Schltze and K. Wippermann, Electrochim. Acta, 32 (1987) 823.
62. H. Ashassi-Sorkhabi, N. Ghalebsaz-Jeddi, F. Hashemzadeh, H. Jahani, Electrochim. Acta, 51 (2006) 3848.
63. R.S. Goncalves, D.S. Azambuja, A.M. Serpa Lucho, Corros. Sci., 44 (2002) 467.
64. E.M. Sherif, S.M. Park, Electrochim. Acta 51 (2006) 1313.
65. H. Ma, S. Chen, S. Zhao, X. Liu, and D. Liu, and D. Li, J. Electrochem. Soc., 148 (2001) B482.
66. O.E. Barcia, O.R. Mattos, N. Pebere, and B. Tribollet, J. Electrochem. Soc., 140 (1993) 2825.
67. H.P. Lee and K. Nobe, J. Electrochem. Soc., 133 (1986) 2035.
68. E. Kraka, D. Cremer, Computer design of anticancer drugs, J. Am. Chem. Soc., 122 (2000) 8245–8264.
69. C. Adamo, V. Barone, Chem. Phys. Lett., 330 (2000) 152–160.
70. M. Parac, S. Grimme, J. Phys. Chem., A 106 (2003) 6844–6850.
71. G. Gece, Corros. Sci., 50 (2008) 2981–2992.
72. R.M. Issa, M.K. Awad, F.M. Atlam, Appl. Surf. Sci., 255 (2008) 2433–2441.
73. Choa, P., Liang, Q., Li, Y., Appl. Surf. Sci., 252 (2005) 1596.
74. N. Khalil, Electrochim. Acta, 48, 2635 (2003).